Characterizing the Sensitivity of a Novel Hall Sensor

Avraham Revah
University of Oklahoma, Norman, Department of Physics
(Dated: May 10^{th}, 2019)

This project aims to characterize the sensitivity of novel Hall sensors for use in the construction of a Hall sensor array with both high spatial and high magnetic field resolution. It looks at three different sized sensors made from an InSb quantum well material: 2mm×2mm, 5mm×5mm, and 10mm×10mm. The sensors achieved a resolution of 20nT, 10nT, and 4nT, respectively. The project also looks at a 10mm×10mm sensor made from an InSb epilayer material; however, no conclusive results for this material were reached. Overall, results indicate the construction of an array with both high spatial and high magnetic field resolution is possible.

I. INTRODUCTION

Hall sensors are devices used for measuring magnetic fields. They have many diverse applications including proximity sensing and geomagnetic navigation. This project is mainly interested in creating an array of Hall sensors with both high spatial ($\sim 100\mu$m) and high magnetic field($\sim 1\mu$T) resolution. These arrays would be useful in the imaging of metallic objects via eddy-current analysis. They may also have uses in certain medical applications, namely magnetocardiography and magnetoencephalography[1, 2].

This project attempts to characterize the magnetic field sensitivity of Hall sensors that will eventually be integrated into a larger array. These sensors were constructed out of InSb using novel techniques in order to achieve high magnetic field resolution. Three of the four sensors investigated fit the proposed model, and their magnetic field resolutions were found to be 20nT, 10nT, and 4nT. However, it is unlikely these sensors would achieve the same resolution in real world applications due to practical limitations. Additionally, more research needs to be conducted to understand why one of the sensors did not fit the proposed model. Nevertheless, these results indicate that constructing an array with both high magnetic field and high spatial resolution should be possible.

II. THEORETICAL BACKGROUND

The Hall Effect is an electromagnetic phenomenon that describes the emergence of a voltage difference across a conductor perpendicular to a supplied bias current and an applied magnetic field. It serves as the foundation for the production of Hall sensors. Figure 1 portrays a simplified version of a Hall effect system. As the carriers flow in response to an applied bias current, they will be deflected by the Lorentz force. These carriers will accumulate on one surface of the conductor and a voltage gradient known as the Hall voltage will develop.

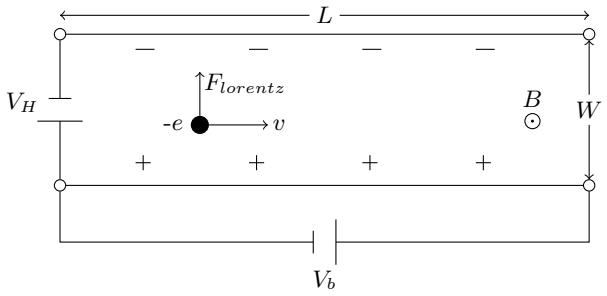

FIG. 1. An idealized depiction of the Hall Effect. As the carriers in the material move in response to the bias voltage, they are deflected by the Lorentz force. As carriers gather on one surface of the material, a voltage gradient called the Hall voltage will develop.

The Hall voltage is given by

$$V_H = gR_H I_B B, \tag{1}$$

where I_B is the supplied bias current and B is the applied magnetic field. R_H is known as the Hall constant and is given by

$$R_H = \frac{1}{en_{2D}}, \tag{2}$$

where e is the fundamental charge and n_{2D} is the two dimensional carrier density of the material. g is a geometric factor dependent on the geometry of the sensor. For a rectangular sensor, it is given by

$$g = \frac{W}{L}, \tag{3}$$

where W is the width and L the length of the sensor[3].

III. DESCRIPTION OF EXPERIMENT

Samples

Equations 1 and 2 indicate the magnitude of the Hall voltage is inversely proportional to n_{2D}. It is likely that

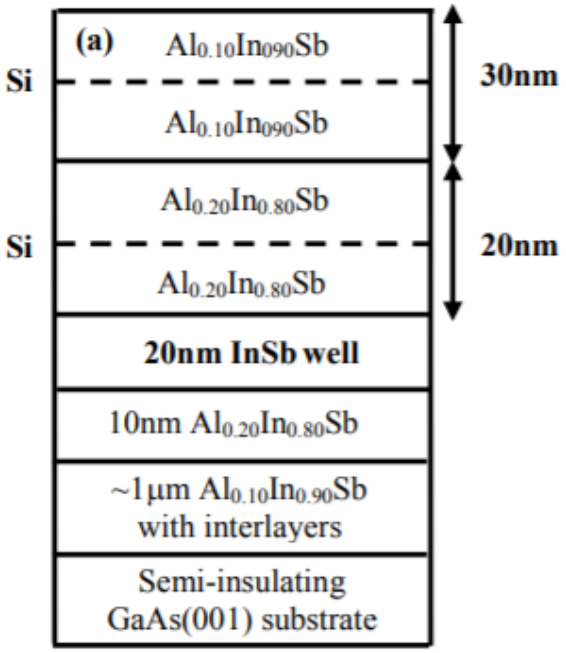

FIG. 2. Depiction of the layer structure for the InSb quantum well material used in this project. The material utilizes remote doping in order to minimize defects. The n_{2D} of this material is $4.10 \times 10^{11}\text{cm}^{-2}$.

maximizing the observed Hall voltage will also minimize error in the measurements. Thus, sensors built out of materials with low n_{2D}'s should outperform sensors built with high n_{2D}'s. To test this hypothesis, two materials with different n_{2D}'s were tested. The first was an InSb quantum well material with a n_{2D} of $4.10 \times 10^{11}\text{cm}^{-2}$. Figure 2 depicts the layer structure for this material. The second was a InSb epilayer material with a n_{2D} of $7.30 \times 10^{12}\text{cm}^{-2}$. Since the epilayer has 20 times the n_{2D} of the quantum well, it should have 20 times the error as well.

Additionally, the sensitivity of the sensors should vary with size. Smaller sensors achieve better spatial resolution, but worse magnetic field resolution. Thus, the error in the magnetic field measurements should vary inversely proportionally with the size of the sensor. In order to test this hypothesis, sensors of three different sizes were tested: 2mm×2mm, 5mm×5mm, and 10mm×10mm.

Apparatus

The Hall sensors were placed in a control circuit designed by Amethyst technologies that amplified the output signal. The circuit was powered by a ±12 volt power supply, and the bias current was supplied by an external current generator. The magnetic field was generated using a coil of wire driven by a lock-in amplifier. The voltage outputted by the control circuit was measured

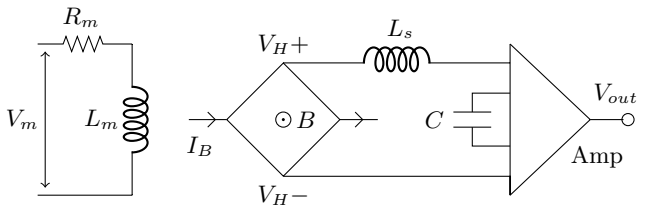

FIG. 3. A schematic detailing the magnet-sensor system. The magnetic field is generated by a coil of inductance L_m, driven by a voltage V_m, and connected to a resistor R_m. The magnetic field is detected by a Hall sensor driven by bias current I_B. The Hall voltage is then modulated by a circuit inductance L_s and an op-amp controlled by a capacitor C. Equations 4 and 5 detail the equations governing this system.

using the lock-in amplifier. The lock-in amplifier was useful in isolating the desired frequency and measuring the phase difference between the applied field and the output voltage. Three times the standard deviation of five measurements was taken to be the error.

Figure 3 shows a schematic detailing the behavior of the experimental system. Using basic circuit analysis and knowledge of the Hall effect, one can deduce the magnitude of the output voltage should be

$$|V_{out}| = \frac{1000\mu_0 N R^2 V_m \sqrt{g^2 R_H^2 I_B^2 + L_s^2\omega^2}}{\sqrt{2}(z^2+R^2)^{3/2}\sqrt{R_m^2+\omega^2 L_m^2}\sqrt{1+(6000\omega C)^2}}, \tag{4}$$

where μ_0 is the permeability of free space, N is the number of loops in the coil, R is the radius of the coil, ω is the frequency of the field, z is the distance from the coil to the sensor, and all other variables are defined in Figure 3 and Equations 1, 2, and 3. Additionally, the phase difference between the output voltage and the applied field should be

$$\begin{aligned}\phi = &-\arctan\left(\frac{L_s}{gR_H I_B}\omega\right) - \arctan\left(\frac{L_m}{R_m}\omega\right) \\ &- \arctan\left(6000\omega C\right),\end{aligned} \tag{5}$$

where all variables have the same meaning as in Equation 4 [3, 4]. In general, many of the constants in Equations 4 and 5 are known. The best way to find them is to fit the model to the data. This was accomplished using the SciPy python library. The code to accomplish this fitting can be found on GitHub[5].

Choosing the Bias Current

Choosing the bias current supplied to the sensors is also a nontrivial problem. If the bias current is too large, the Hall voltage will saturate the op-amp and the output signal will lose all meaning. If the bias current is too small, the Hall voltage will stop varying linearly with bias current as expected by Equation 1. Originally, it

Sample	L_m (mH)	L_s (mH)	C (nF)	Scaling
QW 10mm	23.351	0.116	.108	1.461
QW 5mm	16.148	0.090	.227	2.830
QW 2mm	15.830	0.094	.015	3.220
Epilayer 10mm	7505.997	2.027	30.245	0.955

TABLE I. Table displaying interesting parameters found by fitting data to the model described in Equations 4 and 5. The parameters do not very much across the quantum well devices, but vary greatly for the epilayer device.

appeared that this non-linearity was due to the sensor essentially "turning off" at low bias current; however, further investigation indicated that the control circuit may always be applying a small bias current to the sensor. If this is the case, the model may have to be revised to account for the current. This ambiguity in how the control circuit functions may come to explain some discrepancies in the results. For the experiments in this paper, a bias current of 0.1mA for the 2mm×2mm and 5mm×5mm quantum wells, 1mA for the 10mm×10mm quantum well, and 10mA for the 10mm×10mm epilayer were found to be the most well behaved for each sensor.

IV. ANALYSIS AND DISCUSSION

Table I shows some of the parameters found by fitting the data to the model. The parameters are roughly the same for the quantum well devices and are consistent with an intuitive physical understanding of the system. However, the parameters for the epilayer device are very different from the quantum well devices. This is an indication that the model has more difficulty predicting the behavior of the epilayer material.

Quantum Well Devices

Figure 4 shows how the measured magnetic field behaves versus log frequency. As can be seen, the measured fields and predicted fields agree well with each other. Additionally, the fields decrease with frequency, which aligns with an intuitive understanding of how electromagnets work. Figure 5 shows the phase behavior as a function of log frequency. Here it is less intuitive what the graph should look like, but the measured and predicted values are similar. Then, Figure 6 displays how the observed fields compare to the predicted fields at 1kHz. Again the measured and predicted values agree with each other. Additionally, the measured fields for each sensor tend to have similar values, indicating that each sensor is measuring the same magnetic field across each experiment. As a whole, these results indicate that the model is correctly predicting the behavior of the quantum well samples.

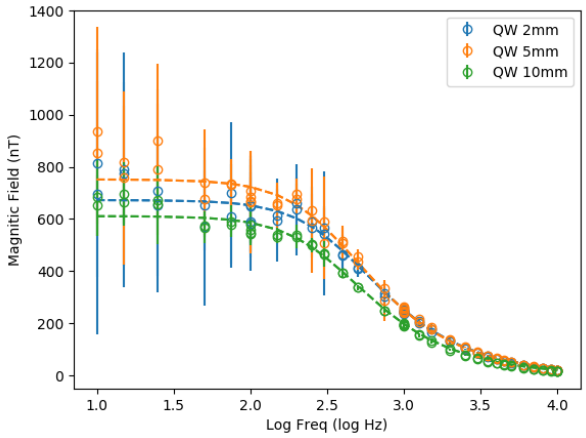

FIG. 4. A plot displaying measured magnetic field versus log frequency for the quantum well devices. The dots represent actual measurements; while, the dotted line represents the predicted behavior. The observations match the expected behavior well, especially at high frequency.

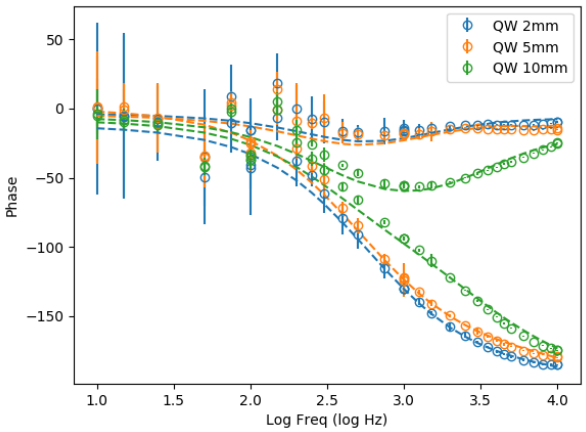

FIG. 5. A plot displaying measured phase versus log frequency for the quantum well devices. The dots represent actual measurements; while, the dotted line represents the predicted behavior. Again, the measured and predicted values match well.

Now that the behavior of the model has been verified, the sensitivity of the sensors can be examined. Figure 7 shows the error in the quantum well measurements as a function of frequency. The error decreases linearly with log frequency before leveling off at around 2nT. This linear dependence may be due to fundamental one over frequency noise in the system; however, it may have more to do with the lock-in amplifier. The lock-in amplifier works by averaging over a time constant(300 ms was used in this project) to extract the Fourier transform of the output signal. At higher frequency, the same time constant will

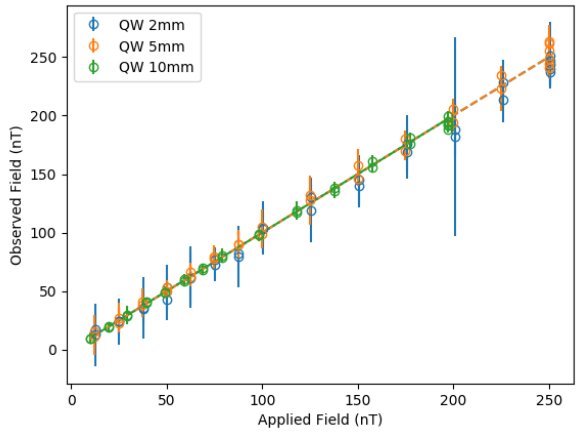

FIG. 6. A plot displaying measured magnetic field versus predicted field for the quantum well devices at 1kHz. The dots represent actual measurements; while, the dotted line represents the predicted behavior. Not only do the measured and predicted values match well, the measured values also match well across the samples. This indicates the same field is being measured by each sample.

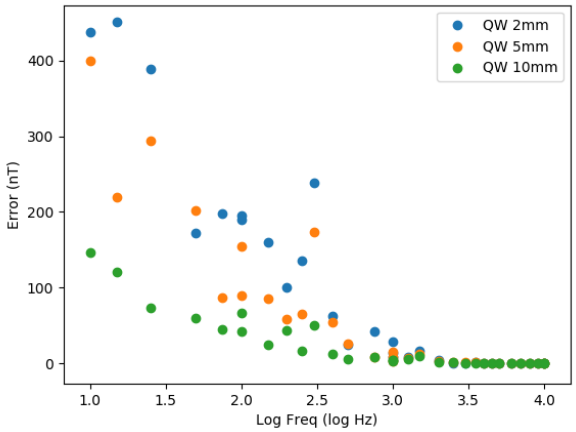

FIG. 7. A plot displaying magnetic field error versus log frequency for the quantum well devices. The error decreases linearly with log frequency at low frequency and levels off at high frequency. Additionally, the order from highest error to lowest error is 2mm sensor, 5mm sensor, and then 10mm sensor as expected.

Sample	Error (nT)
QW 2mm	20
QW 5mm	10
QW 10mm	4

TABLE II. Table displaying average error for quantum well devices at 1kHz.

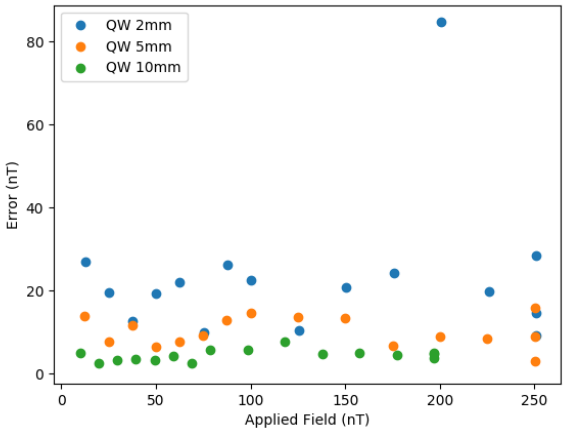

FIG. 8. A plot displaying magnetic field error versus measured magnetic field for the quantum well devices at 1kHz. The average errors for the devices can be found in Table II and follow the expected trend.

capture more cycles and should produce better data[6]. Either way, error decreasing linearly with frequency is not unexpected. The leveling off of the error at high frequency is likely due to error from some other component dominating when the frequency dependent error is small. This could be due to the minimum resolution of the lock-in amplifier or a noisy component. Additionally, the hypothesized error dependence on sensor size is supported by Figure 7. The 2mm×2mm device has the most error, the 10mm×10mm device has the least, and the 5mm×5mm is in between them. Figure 8 shows the error versus applied field for the quantum well devices at 1kHz. The error remains relatively constant for all fields, which is not surprising. Additionally, the errors seem to decrease linearly with the size of the sensor as expected. Table II shows the average error for each device at 1 kHz. The errors follow the expected one over size dependence very nicely.

Epilayer Device

Figure 9 shows the measured and predicted fields as functions of log frequency for the 10mm×10mm epilayer device. In this case, the observed and predicted values do not match well at all. Additionally, the field is much smaller than the field measured for the quantum wells in Figure 4, but nothing about the magnet was changed in between the experiments. This is a strong indication that the model fails to correctly predict the behavior of the epilayer device.

Figure 10 displays the error in the magnetic field measurements as a function of frequency for the 10mm×10mm epilayer device. The error was expected to be 20 times larger than the error for the quantum well

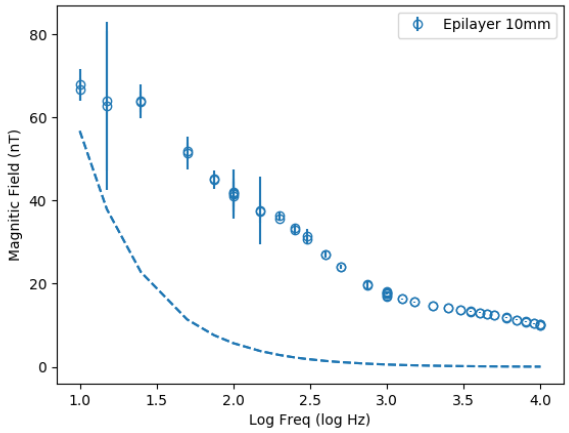

FIG. 9. A plot displaying measured magnetic field versus log frequency for the epilayer device. The dots represent actual measurements; while, the dotted line represents the predicted behavior. The measured values do not match the predicted values. This is an indication that the model fails to fit the data in the epilayer case.

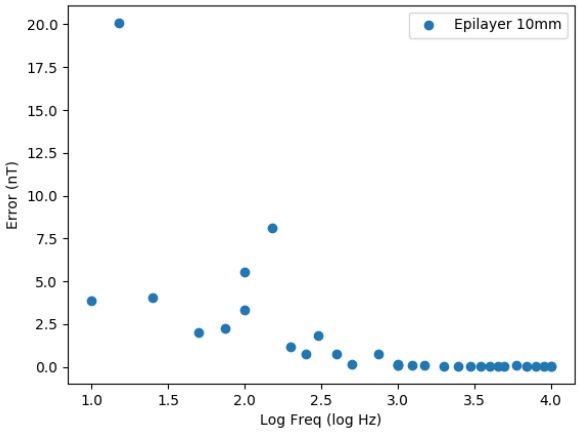

FIG. 10. A plot displaying magnetic field error versus log frequency for the epilayer device. The measured error is much smaller than expected. This is another indication that the model fails to fit the epilayer data.

devices, but it is much smaller. This implies that the model does not fit the behavior of the epilayer.

There are several reasons the model may fail to predict the behavior of the epilayer well. First of all, the model is brittle, meaning its convergence is very dependent on the initial guesses for each parameter. It is possible that better initial parameters may allow the model to converge to a better solution. However, this possibility unlikely as there is no reason to believe the parameters for the epilayer should vary wildly from the parameters for the quantum wells. The most likely reason the model fails may have to do with the bias current applied to the epilayer device. A much larger bias current was applied to the epilayer than to the quantum wells in these experiments. This was done because the epilayer did not behave as expected at low bias current. It is possible that the control circuit may be applying a small bias current on top of the external bias current. This would throw off the model and may disproportionately affect the epilayer device.

V. CONCLUSION

The model of the system described in this paper is able to accurately predict the behavior of the quantum well devices. Using this model, we found the sensitivity for the 2mm×2mm, 5mm×5mm, and 10mm×10mm devices to be 20nT, 10nT, and 4nT, respectively. However, the model was not able to accurately predict the behavior of the epilayer device. More investigation is necessary to determine why, but it likely has to do with the bias current being supplied to the system.

The results of this project indicate that the InSb quantum well Hall sensors used do indeed have high magnetic field resolution. It is unlikely these sensors would be able to achieve the same resolution in real world settings because of limitations on the supplied bias current and time constant for each measurement. However, their sensitivity should still be very good. Ultimately, it should be possible to construct sensor arrays with high spatial and high magnetic field resolution out of the quantum well sensors.

[1] D. Pappas, "High sensitivity magnetic field sensor technology overview," National Institute of Standards and Technology (2008).
[2] P. Ripka, Journal of Physics: Conference Series **450** (2013).
[3] D. J. Griffiths, *Introduction to electrodynamics* (Cambridge University Press, 2017).
[4] J. Lindemuth and S. Mizuta, Thin Film Solar Technology III (2011).
[5] A. Revah, "Github repository," github.com/aar015/hall-sensors (2019).
[6] *MODEL SR830 DSP Lock-In Amplifier*.